Check for updates

Investigation on binary copper-based catalysts used in the ethanol steam reforming process

Łukasz Hamryszak[1] [ORCID] **· Maria Madej-Lachowska[2] · Maria Kulawska[1] · Małgorzata Ruggiero-Mikołajczyk[3] · Katarzyna Samson[3] · Michał Śliwa[3]**

Abstract

The use of copper-based binary catalysts, Cu/Zr oxides and Cu/Al oxides, has been examined to produce hydrogen from ethanol in the ethanol steam reforming process. The examined catalysts were compared with non-noble bicomponent catalysts consisting of oxides of nickel and cobalt: Ni/Zr Co/Zr, Ni/Al and Co/Al, prepared and tested in the identical way. Catalytic tests were carried out in the fixed-bed reactor in the temperature range 433–873 K for initial molar ratio of ethanol to water equal to 1:3. Ethanol conversion approached near 100%. Catalysts were characterized by XRD, TPR. Cu/Zr oxides. The catalyst showed very good selectivity. It is significant that carbon monoxide appeared only above 600 K and its selectivity has not exceeded 3% in the higher temperature range. No methane has been detected. Hydrogen yield was relatively stable in the temperature range from 513 to 873 K. Similarly, in the presence of Cu/Al oxides neither CO nor CH_4 were found in the products. The correlation between activity of examined catalysts and textural properties was not found.

✉ Łukasz Hamryszak
  lukasz.hamryszak@interia.pl

[1] Institute of Chemical Engineering, Polish Academy of Sciences, 5 Bałtycka Street, 44-100 Gliwice, Poland

[2] Opole University of Technology, 31 Sosnkowskiego Street, 45-272 Opole, Poland

[3] Jerzy Haber Institute of Catalysis and Surface Chemistry, Polish Academy of Sciences, 8 Niezapominajek Street, 30-239 Kraków, Poland
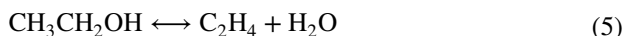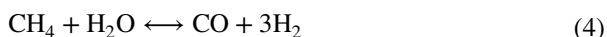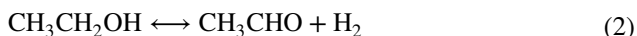
Introduction

The increase in environmental pollution and new restrictions and regulations require new clean technologies of high energy efficiency, so the search for alternative sources of green energy. Nowadays there is no doubt that hydrogen is the most important carrier of clean energy [1]. Until today, it was produced in industry from gasification of coal and other fossil materials, in steam reforming of hydrocarbons (mainly methane) and oxygenates (mainly methanol) [2, 3] and from electrolysis of water [4]. In last two decades ethanol steam reforming is of great interest because ethanol is safe and easy in storage and distribution. There are many sources of cheap ethanol like biomass and all substrates with starch content [5].

The main reaction of hydrogen production process from ethanol is strong endothermic [1]:

$$C_2H_5OH \; + \; 3H_2O \; \longleftrightarrow \; 2\,CO_2 + \; 6\,H_2 \quad \Delta H_{298} = +174\,\text{kJ/mol} \qquad (1)$$

Many side reactions occur in the ethanol steam reforming process forming undesired products as carbon monoxide, methane, acetic acid, acetaldehyde, ethene and others [6].

$$CH_3CH_2OH \longleftrightarrow CH_3CHO + H_2 \qquad (2)$$

$$CH_3CHO \longleftrightarrow CH_4 + CO \qquad (3)$$

$$CH_4 + H_2O \longleftrightarrow CO + 3H_2 \qquad (4)$$

$$CH_3CH_2OH \longleftrightarrow C_2H_4 + H_2O \qquad (5)$$

$$C_2H_4 \longleftrightarrow 2C + 2H_2 \qquad (6)$$

$$C_2H_4 + 2H_2O \longleftrightarrow 2CO + 4H_2 \qquad (7)$$

It is known that even a little improvement in hydrogen selectivity and lowering of concentration of carbon monoxide in the product is very important because of poisoning effect of this in fuel cells. CO is a strong poison for PEFC anode catalysts, the system cannot accept more than 100 ppm for efficient operation [5]. The methane has no negative effect on the anode, it can be used to provide heat for the endothermic reforming process [7]. As is evident, this is a process with a very complex mechanism, and therefore requires active and selective catalysts operating under severe conditions. At the same time it must be resistant to carbon deposition on the catalyst surface (coking) [8].

Up to now the noble metal (rhodium, platinum, ruthenium or iridium) catalysts have been applied in this process with good results [9–12]. Due to the high cost of precious metals, numerous efforts are undertaken to develop cheaper catalysts with comparable properties.

The properties of catalysts depend mainly on their composition, especially on active metal content and support type, but also on all parameters of preparation. Most of the studies concern on nickel [5, 13–22] and cobalt [7, 8, 15, 16, 18–20, 23–28] based catalysts. In the literature available studies on nickel catalysts, the nickel content varies from 5 to 20 mass% deposited on various supports [5, 22]. These catalysts are active in the ethanol steam reforming in the temperature range 573–923 K [1], with an optimal nickel content of about 10 mass% [14, 16, 17]. Extensive research has been conducted on a number of different supports, of which oxides of Ti [16], Si Mg [13], La [15] and Zn [17] deserve attention. The studies on cobalt-based catalysts with a content of cobalt from 2 to 18 mass% [7, 8, 15, 16, 18–20, 23–28] show increase in their activity with an increase of its content in the temperature range from 623 to 773 K [1, 27]. Oxides of Zn, Ce, Sm, La [23] and Al [24] are listed as optimal supports for these catalysts.

An important problem concerning ethanol steam reforming process is catalyst deactivation caused by coking. Increase in acidity of active centres of the support gives decrease in activity because of increasing tendency to formation of carbon deposits (coking) [5] which main source is the dehydrogenation of ethanol followed by decomposition of ethene [6]. According to Padilla et al. [20] lanthanum addition causes gasification of deposited coke. The elimination of coking can be also realized by using of stoichiometric excess of water to ethanol from 2 to 18 [5].

There are not many works concerning catalysts based on copper. According to Rossetti et al. [16], those deposited on TiO_2 show high resistance to coking. However, they exhibit poor ability to break the C–C bonds, therefore acetaldehyde and ethylene predominate in the products; it indicates that the main source of hydrogen is the reaction of their dehydrogenation. Bergamaschi et al. [21] found the high catalyst activity of Ni/Cu = 8/3 mass% complex supported on ZrO_2. Vizcaíno et al. [6] found that in Cu/Ni catalyst supported on SiO_2 nickel is the phase responsible for hydrogen production while copper—for decrease both in CO formation and coke deposition.

There are great differences in reported works concerning active metal content and the tested parameters, especially in terms of steam excess. For this reason, it is very difficult to select the optimal catalyst composition on the base on literature data.

The aim of this work is to study the applicability of Cu/Zr oxides and Cu/Al oxides binary catalysts to produce hydrogen from ethanol. The activities of the tested Cu/Zr oxides and Cu/Al oxides catalysts were compared to those of nickel (Ni/Zr and Ni/Al) and cobalt (Co/Zr and Co/Al) oxides catalysts prepared by the same method and tested in the identical conditions.

Experimental

Materials

For the synthesis of catalysts: $Ni(NO_3)_2 \cdot 6H_2O$, $Co(NO_3)_2 \cdot 6H_2O$, $Cu(NO_3)_2 \cdot 3H_2O$, $ZrO(NO_3)_2 \cdot H_2O$, purchased from Sigma-Aldrich Poland; citric acid monohydrate purchased from Stanlab Sp.j. Poland; 65 mass% nitric acid, purchased from

Avantor Performance Materials Poland; all of AR grade. To determine activity: ethanol Merck KGaA, gradient grade for liquid chromatography.

Catalysts synthesis

All catalysts have been prepared according to the method described by Courty et al. [29]. The method of complex formation of metals by citric acid and thermal decomposing the citrate complexes proved the best in our laboratory. The mixture is perfectly mixed because of branched structure of citrates. The use of citrate complexes gave excellent homogeneity and fully repeatable properties of the prepared catalyst [30], while the conventional method of co-precipitation did not provide such results, although the latter is usually used, as is known from the literature. The formed catalysts were calcinated in a muffle at temperature 623 K. In all obtained catalysts the ratio of metal (Ni, Co, Cu) oxide to alumina or zirconia, respectively, was the same, equal to 63.8/36.2 (mass%/mass%).

Catalysts characterization

Phase analysis based on X-ray powder diffraction (XRD) measurements was performed on a X'PERT PRO MDP diffractometer with detector X'CELERATOR, working in Bragg–Brentano geometry. The XRD measurements (at 40 kV and 30 mA) were performed in the 2 h range from 5° to 90° with the interpolated step size 0.02°. The crystallite sizes were calculated from Scherrer method. XRD phase analysis was performed using reference standards from the International Centre for Diffraction Data (ICDD) PDF-4 database.

The specific surface area (S_{BET}) and porosity of catalysts were determined with the Multi-Point BET Plot analysis method using an Autosorb-1 Quantachrome apparatus, with nitrogen as an adsorbate at 77 K. Prior to the measurements, the samples were preheated and degassed under vacuum at 373 K for 18 h. The micropore area was obtained by V-t plot method t-micropore analysis while pore size distribution was calculated with the BJH method.

H_2-TPR (temperature-programmed reduction of H_2) measurements were performed in Chembet-3000 (Quantachrome) u-shape quartz flow reactor (diameter ca. 5 mm) at temperature range 300–1050 K with temperature ramp of 10 K/min and a flow rate of 5% H_2 in Ar. Before the TPR analysis, all samples were kept in a stream of helium at 373 K for 1.5 h to remove physically adsorbed water.

Size of crystallites of tested catalysts are presented in Table 1. Catalyst composition and textural properties are presented in Table 2.

Catalytic tests

A continuous fixed-bed reactor of 8 cm^3 volume, made of stainless steel, was used in the catalytic experiments. The bed consisted of 2 g of the catalyst of grain size of 0.8–1.0 mm. The catalyst was reduced in a stream of diluted hydrogen (7% H_2 in N_2) at 723 K under atmospheric pressure for 4 h and activated in the mixture of the reactants

Table 1 Sizes of crystallites of tested catalysts

Catalyst	Size of crystallites (nm)					
	Ni (111)	Co (111)	CoO (111)	Cu (111)	Cu$_2$O (111)	ZrO$_2$ (111)
Ni/Zr oxides	12.8	–	–	–	–	8.4
Co/Zr oxides	–	11.8	3.3	–	–	10.3
Cu/Zr oxides	–	–	–	23.2	–	5.5
Ni/Al oxides	8.1	–	–	–	–	–
Co/Al oxides	–	–	–	–	–	–
Cu/Al oxides	–	–	–	22.5	7.5	–

Table 2 Composition and textural properties of tested catalysts

Catalyst	Main metal (mass%)	Zirconia/aluminia (mass%)	S_{BET} (m^2/g)	V_p (cm^3/g)	D_p (nm)
Co/Zr oxides	63.8	36.2	89	0.16	7
Cu/Zr oxides	63.8	36.2	23	0.07	13
Ni/Al oxides	63.8	36.2	146	0.18	5
Co/Al oxides	63.8	36.2	27	0.15	22
Cu/Al oxides	63.8	36.2	13	0.04	13

at 473 K for 4 h. The catalytic activity in the ethanol conversion was determined under the following conditions: atmospheric pressure, temperature range dependent on catalyst activity within 433–873 K, space velocity of the reactants flow 100 ml/min, initial molar ratio of ethanol to water equal to 1:3 under pure N$_2$ flow. The feed gas was deoxidized with the BTS deoxidizer and dehydrated with the molecular sieve 5 Å. Substrates and products were directed on-line to chromatograph Varian Star 3800. Then the gases were decompressed to the atmospheric pressure and cooled to separate the liquid fraction. The gaseous products were analyzed in the system of Carbo Plot P7 column, 25 m 0.53 mm and Supelcowax 10 column, 30 m·0.32 mm. Ethanol was determined quantitatively in the Supelcowax 10 column and FID detector and the remaining gases in the Carbo Plot P7 column and TCD detector. Additionally carbon monoxide and methane were determined quantitatively in the methanizer with the sensitivity of 20 ppb [31]. Time on stream was between 23 and 36 h.

Activity of tested catalysts was characterized by hydrogen yield, ethanol conversion and selectivities of carbon monoxide and methane according to formulas given below [32]:

$$W_{H_2} = \frac{V_{H_2}}{m_{cat.}} \quad (L/kg_{cat.} \cdot h) \tag{8}$$

$$\alpha = \frac{F_{Et}^{in} - F_{Et}^{out}}{F_{Et}^{in}} 100 (\%) \tag{9}$$

$$S_i = \frac{F_i^{out}}{2\left(F_{Et}^{in} - F_{Et}^{out}\right)} 100\% \tag{10}$$

Here $m_{cat.}$ (g) is the catalyst mass, V_{H_2}(L/h) is the volume flow rate, F_i^{in} and F_i^{out} (mol/h) is the molar flow rate of i-th component at input (EtOH) and output (CO, CH$_4$), respectively.

Results and discussion

The phase composition of prepared catalysts was determined by XRD investigations presented in Fig. 1. The phase analysis revealed a presence of dominant peaks between $2\theta = 40$–$44°$ connected to Ni^0, Co^0 and Cu^0. Some of the peaks of weak intensity observed in samples of catalysts containing zirconia were caused by its crystallization (Fig. 1a). Other peaks were connected to CoO. For the Co/Al oxides catalyst it was not possible to fit phases (Fig. 1b) because of low intensity of signals, so the description of reflexes missed. Other peaks in Fig. 1b were connected to NiO and Cu$_2$O. No Al$_2$O$_3$ and mixed metal/zirconia as well as metal/alumina phases were detected. The crystallite sizes of the Ni^0, Co^0 or Cu^0 are different. Calculation of crystallite size of Co/Al oxides catalyst by Scherrer method (Table 1) was not possible.

Values of specific surface area BET, pore volume and average pore diameter are presented in Table 2. Specific surface area and total pore volume (V_p) decreased in following order: Ni/Al > Ni/Zr > Co/Zr > Co/Al > Cu/Zr > Cu/Al oxides. The Ni/Zr oxides and Ni/Al oxides catalysts revealed the highest values of S_{BET} and V_p over 10 times higher than those of Cu/Zr oxides and Cu/Al oxides (Table 2). The value of total pore volume of obtained catalysts reached about 0.2 cm^3/g. There was found correlation between specific surface area and value of
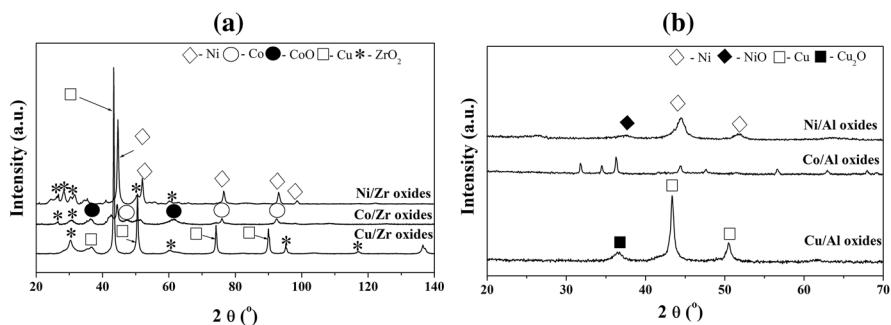

Fig. 1 XRD patterns of tested catalysts

crystallite size of active metal (see Tables 1, 2). The Cu/Zr oxides and Cu/Al oxides catalysts revealed the lowest values of specific surface area (23 m^2/g and 13 m^2/g respectively) and the highest values of crystallite sizes of Cu^0 (23.3 nm and 22.5 nm respectively).

H$_2$–TPR profiles of investigated catalysts are presented in Fig. 2. Ni/Zr oxides catalyst showed broad peaks: low-temperature one with maximum at 662 K and high-temperature one with maximum at 799 K. The first one is responsible for reduction of NiO to Ni^0, the second one—for reduction of strongly dispersed NiO in Zr oxide [19]; it was not proved by XRD investigations. TPR profile of Ni/Al oxides catalyst revealed a single very broad reduction peak at higher temperature of 820 K comparing with Ni/Zr oxides catalyst. TPR profiles of Co/Zr oxides and Co/Al oxides catalysts revealed 3 reduction peaks of various intensity, two low-temperature ones at 627 K (Co/Al oxides), 631 K (Co/Zr oxides) and 671 K (Co/Al oxides), 682 K (Co/Zr oxides). High-temperature maximum was observed at 771 K and 938 K, respectively. The first peaks were connected with two-stage reduction of Co$_3$O$_4$ to CoO and to Co^0. The last peak was connected with reduction of CoO strongly connected with Zr oxide or Al oxide [7, 20]. Co/Al oxides catalyst was reduced at lower temperatures than Co/Zr oxides. Cu/Zr oxides catalyst was reduced from CuO to Cu^0, it revealed strong single peak at 582 K [33]. Cu/Al oxides catalyst was reduced at temperature about 30 K higher than Cu/Zr oxides catalyst. A broad peak was observed, which contained reduction of CuO to Cu$_2$O followed by reduction to Cu^0; it was proved by XRD investigations. As shown by the H$_2$–TPR profile, the Cu/Al catalyst is fully reduced to Cu^0 at 617 K. On the other hand, on the XRD spectra, there is a relatively intense Cu$_2$O reflex, which may indicate its partial oxidation after the reaction (Figs. 1b, 2b).

Catalytic activity results are presented graphically in Figs. 3, 4, 5 and 6 and Table 3.

All catalysts achieved a high degrees of conversion (Fig. 3a, b).

Zirconia containing catalysts (Figs. 3a, 4a, 5a, 6a).

Ni/Zr oxides catalyst reaches the highest hydrogen yield of − 756 L/(kg$_{cat.}$ h) at 773 K, unfortunately accompanied by high production of carbon monoxide (selectivity 13%) and methane (selectivity about 32%).
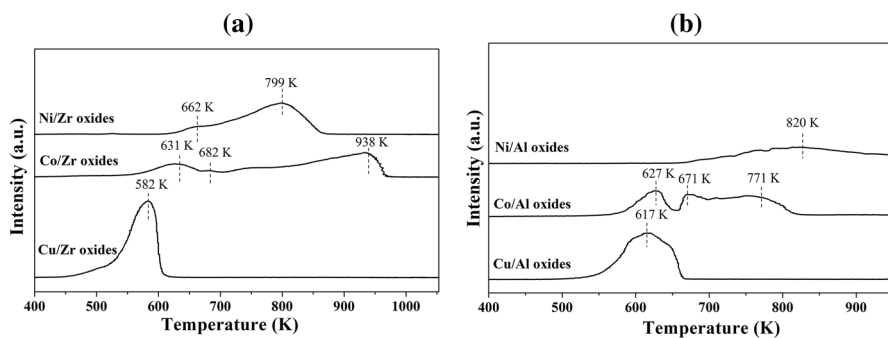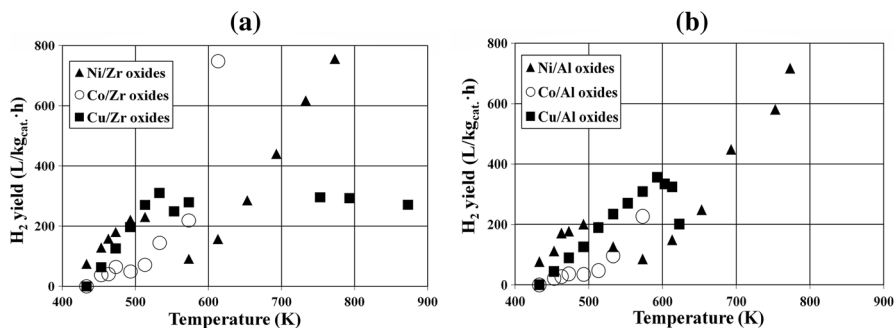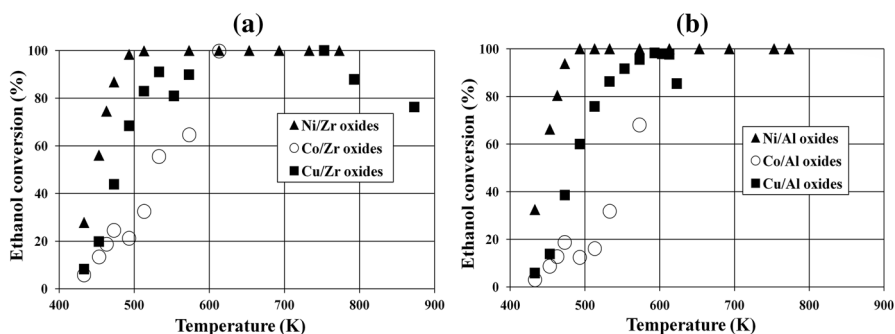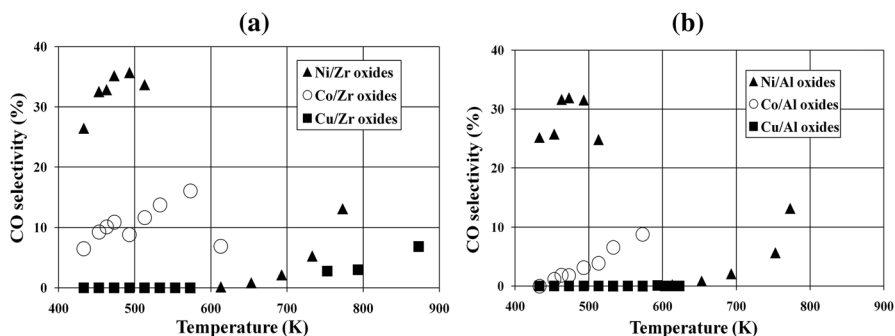

Fig. 2 H$_2$-TPR profiles of tested catalysts

(a) **(b)**

Fig. 3 H_2 yield as a function of the temperature for **a** zirconia and **b** alumina containing catalysts
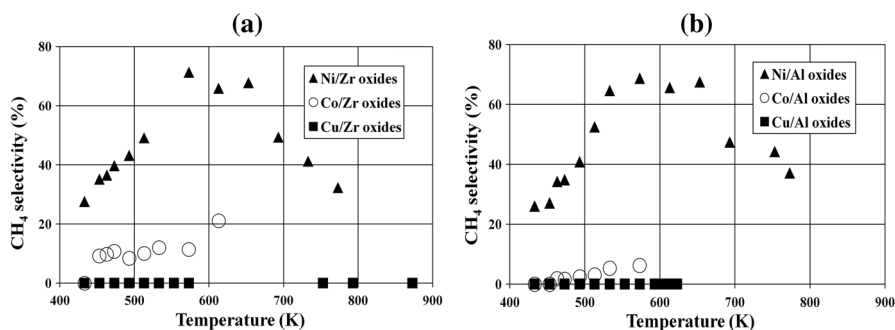
(a) **(b)**

Fig. 4 Ethanol conversion as a function of the temperature for **a** zirconia and **b** alumina containing catalysts

(a) **(b)**

Fig. 5 CO selectivity as a function of temperature for **a** zirconia and **b** alumina containing catalysts

Co/Zr oxides catalyst reaches a little lower hydrogen yield of 748 L/(kg$_{cat.}$ h) than Ni/Zr oxides catalyst, but at lower temperature of 613 K (Fig. 3a). In the range of 433–573 K carbon monoxide and methane selectivities increase with the temperature. Further increase in temperature causes rapid decrease in carbon

Fig. 6 CH_4 selectivity as a function of for **a** zirconia and **b** alumina containing catalysts

Table 3 Maximum hydrogen yield at corresponding temperature for tested catalysts

Catalyst	T (K)	(L/kg$_{cat.}$ h)	α (%)	S$_{CO}$ (%)	(%)
Ni/Zr oxides	773	756	100	13	32
Co/Zr oxides	613	748	100	7	21
Cu/Zr oxides	533	309	91	0	0
Ni/Al oxides	773	717	100	13	37
Co/Al oxides	573	227	68	9	6
Cu/Al oxides	593	356	98	0	0

monoxide selectivity to 7% and increase in methane selectivity to 21% at 613 K (Figs. 5a, 6a).

It is worth emphasizing the fact that the Cu/Zr oxides catalyst showed very good selectivity. Hydrogen yield in the temperature range 513–873 K remained relatively stable but significantly lower − 271 L/(kg$_{cat.}$ h) than over the Co/Zr oxides and Ni/Zr oxides catalysts at 613 K and 773 K respectively (Fig. 3a). In the hydrogen output stream, carbon monoxide appeared above 600 K and its selectivity did not exceed 3% in the higher temperature range (Fig. 5a). No CH_4 has been detected (Fig. 6a).

Alumina containing catalysts (Figs. 3b, 4b, 5b, 6b).

Ni/Al oxides catalyst showed similar to Ni/Zr oxides hydrogen yield (717 L/(kg$_{cat.}$ h)) and CO selectivity of 13% with a CH_4 selectivity about 35% at 773 K (Table 3). Unfortunately, this catalyst has become sintered. Taking into account the hydrogen efficiency, selectivities towards by–products (carbon monoxide and methane) and sintering of the catalyst, hydrogen production should be carried out at temperatures below 753 K (Figs. 5b, 6b).

Co/Al oxides catalyst compared to Co/Zr oxides showed a slightly higher hydrogen yield (227 L/(kg$_{cat.}$·h)) as well as over two times lower CO selectivity (8%) and almost twice lower CH_4 selectivity (6%) at 573 K (Table 3). Similarly to the Ni/Al oxides catalyst, it has become deactivated, so the process should be carried out at temperatures below 613 K.

Cu/Al oxides catalyst showed a higher hydrogen yield of 309 L/(kg$_{cat.}$ h) at 573 K than Cu/Zr oxides (Fig. 3a, b). Above this temperature the yield reached its

maximum and then rapidly decrease. Similarly to Cu/Zr oxides catalyst, neither CO nor CH_4 were found in the products (Figs. 5b, 6b).

Experimental results are collected in Table 3. The tested catalysts achieved their activity toward hydrogen production for different temperature ranges, therefore the table shows the maximum hydrogen efficiencies and corresponding temperatures.

The correlation between activity of examined catalysts and textural properties was not found. The only relationship that has been found is between pore diameter and hydrogen yield: about 50% increase in pore diameter caused a decrease in hydrogen yield (see Table 2).

There was found, that decrease in crystallite sizes of the Ni^0, Co^0 phase gave an improvement of its dispersion followed by high hydrogen yield (Fig. 1, Table 1). Ni/Al oxides catalyst had the highest values of specific surface area BET (146 m^2/g) and total pore volume (0.18 cm^3/g) and the lowest values of crystallite sizes of the Ni^0 (8.1 nm). Large crystallites and large pore diameters of Cu/Zr oxides and Cu/Al oxides catalysts could be responsible for the agglomeration of metal therefore giving low values of specific surface area BET and total pore volume and in effect low values of hydrogen yield (Tables 1, 2, 3).

Based on TPR and test results, the lower hydrogen reduction temperature corresponds to the lower temperature at which the catalysts achieve maximum hydrogen efficiency (Fig. 2, Table 3). In the case of Cu/Zr oxides and Cu/Al oxides catalysts, the H_2–TPR peaks at lower reduction temperatures were connected with large crystallites that caused decreased dispersion (Fig. 2, Table 1).

Summary

This paper presents studies on the activity of Cu/Zr oxides and Cu/Al oxides catalysts in the ethanol steam reforming process. Their activity was compared with Ni/Zr, Co/Zr, Ni/Al and Co/Al. The Ni/Zr oxides catalyst, characterized by high hydrogen efficiency of 756 L/($kg_{cat.}$ h) at 100% ethanol conversion at 773 K, appeared to be the best catalyst among the ones investigated by us in the steam reforming process. The copper catalysts (Cu/Zr oxides and Cu/Al oxides) showed lower hydrogen efficiency (309 L/($kg_{cat.}$ h) at 533 K and 356 L/($kg_{cat.}$ h) at 593 K, respectively), but their significant advantage is the lack of CO formation, which is of a great importance in the aspect of using the produced hydrogen in fuel cells.

The correlation between activity of examined catalysts and textural properties was not found. The only relationship that has been found is between pore diameter and hydrogen yield: about 50% increase in pore diameter caused a decrease in hydrogen yield.

The attempts to apply bicomponent copper-based catalysts (Cu/Al oxides and Cu/Zr oxides) in the ethanol steam reforming process showed their excellent selectivity and good resistance to coking. However, they revealed unsatisfactory activities due to low hydrogen yields. It seems reasonable to continue investigations to modify the chosen Cu/Zr oxides catalyst in order to obtain higher hydrogen efficiency. Some promoters will be tested.

References

1. Ogo S, Sekine Y (2020) Recent progress in ethanol steam reforming using non-noble transition metal catalysts: a review. Fuel Process Technol 199:106238–106249. https://doi.org/10.1016/j.fuproc.2019.106238
2. Gonzalez-Gil R, Chamorro-Burgos I, Herrera C, Larrubia MA, Laborde M, Marino F, Alemany LJ (2015) Production of hydrogen by catalytic steam reforming of oxygenated model compounds on Ni-modified supported catalysts. Simulation and experimental study. Int J Hydrogen Energy 40:11217–11227. https://doi.org/10.1016/j.ijhydene.2015.05.167
3. Madej-Lachowska M, Kulawska M, Słoczyński J (2017) Methanol as a high purity hydrogen source for fuel cells: a brief review of catalysts and rate expressions. Chem Proc Eng 38:147–162. https://doi.org/10.1515/cpe-2017-0012
4. Rashid MM, Al Mesfer MK, Naseem H, Danish M (2015) Hydrogen production by water electrolysis: a review of alkaline water electrolysis, PEM water electrolysis and high temperature water electrolysis. Int J Eng Adv Technol 4:80–93
5. Ni M, Leung DYC, Leung MKH (2007) A review on reforming bio-ethanol for hydrogen production. Int J Hydrogen Energy 32:3238–3247. https://doi.org/10.1016/j.ijhydene.2007.04.038
6. Vizcaino AJ, Carrero A, Calles JA (2007) Hydrogen production by ethanol steam reforming over Cu–Ni supported catalysts. Int J Hydrogen Energy 32:1450–1461. https://doi.org/10.1016/j.ijhydene.2006.10.024
7. Batista MS, Santos RKS, Assaf EM, Assaf JM, Ticianelli EA (2004) High efficiency steam reforming of ethanol by cobalt-based catalysts. J Power Sources 134:27–32. https://doi.org/10.1016/j.jpowsour.2004.01.052
8. Augusto BL, Ribeiro MC, Aires FJCS, da Silva VT, Noronha FB (2018) Hydrogen production by the steam reforming of ethanol over cobalt catalysts supported on different carbon nanostructures. Today Catal. https://doi.org/10.1016/j.cattod.2018.10.029
9. Sharma PK, Saxena N, Roy PK, Bhat A (2016) Hydrogen generation by ethanol steam reforming over Rh/Al$_2$O$_3$ and Rh/CeZrO$_2$ catalysts: a comparative study. Int J Hydrogen Energy 41:6123–6133. https://doi.org/10.1016/j.ijhydene.2015.09.137
10. Frusteri F, Freni S, Spadaro L, Chiodo V, Bonura G, Donato S, Cavallaro S (2004) H$_2$ production for MC fuel cell by steam reforming of ethanol over MgO supported Pd, Rh, Ni and Co catalysts. Catal Commun 5:611–615. https://doi.org/10.1016/j.catcom.2004.07.015
11. Palma V, Castaldo F, Ciambelli P, Iaquaniello G (2014) H2 production for MC fuel cell by steam reforming of ethanol Over MgO supported Pd, Rh, Ni and Co catalysts. Appl Catal B Environ 145:73–84. https://doi.org/10.1016/j.apcatb.2013.01.053
12. Jia H, Zhang J, Yu J, Yang X, Sheng X, Xu H, Sun Ch, Shen W, Goldbach A (2019) Efficient H$_2$ production via membrane-assisted ethanol steam reforming over Ir/CeO$_2$ catalyst Int. J Hydrogen Energy 44:24733–32475. https://doi.org/10.1016/j.ijhydene.2019.07.199
13. Fajardo HV, Longo E, Mezalira D, Nuernberg G, Almerindo G, Collasiol A, Probst LFD, Garcia ITS, Carreño NLV (2010) Influence of support on catalytic behavior of nickel catalysts in the steam reforming of ethanol for hydrogen production. Environ Chem Lett 8:79–85. https://doi.org/10.1007/s10311-008-0195-5
14. Araiza DG, Gómez-Cortés A, Díaz G (2018) Effect of ceria morphology on the carbon deposition during steam reforming of ethanol over Ni/CeO$_2$ catalysts. Catal Today. https://doi.org/10.1016/j.cattod.2018.03.016

15. Fatsikostas AN, Kondarides DI, Verykios XE (2002) Production of hydrogen for fuel cells by reformation of biomass-derived ethanol. Catal Today 75:145–155. https://doi.org/10.1016/S0920-5861(02)00057-3

16. Rossetti I, Lasso J, Finocchio E, Ramis G, Nichele V, Signoretto M, Di Michele A (2014) TiO2-supported catalysts for the steam reforming of ethanol. Appl Catal A Gen 477:42–53. https://doi.org/10.1016/j.apcata.2014.03.004

17. Yang Y, Ma J, Wu F (2006) Production of hydrogen by steam reforming of ethanol over a Ni/ZnO catalyst. Int J Hydrogen Energy 31:877–882. https://doi.org/10.1016/j.ijhydene.2005.06.029

18. Pinton N, Vidal MV, Signoretto M, Martínez-Arias A, Cortés Corberán V (2017) Ethanol steam reforming on nanostructured catalysts of Ni, Co and CeO2: influence of synthesis method on activity, deactivation and regenerability. Catal Today 296:135–143. https://doi.org/10.1016/j.cattod.2017.06.022

19. Li S, Li M, Zhang Ch, Wang S, Ma X, Gong J (2012) Steam reforming of ethanol over Ni/ZrO2 catalysts: effect of support on product distribution. Int J Hydrogen Energy 37:2940–2949. https://doi.org/10.1016/j.ijhydene.2011.01.009

20. Padilla R, Benito M, Rodriguez L, Serrano A, Munoz G, Daza L (2010) Nickel and cobalt as active phase on supported zirconia catalysts for bio-ethanol reforming: influence of the reaction mechanism on catalysts performance. Int J Hydrogen Energy 35:8921–8928. https://doi.org/10.1016/j.ijhydene.2010.06.021

21. Bergamaschi VS, Carvalho FMS, Rodrigues C, Fernandes DB (2005) Preparation and evaluation of zirconia microspheres as inorganic exchanger in adsorption of copper and nickel ions and as catalyst in hydrogen production from bioethanol. Chem Eng J 112:153–158. https://doi.org/10.1016/j.cej.2005.04.016

22. Sharma YC, Kumar A, Prasad R, Upadhyay SN (2017) Ethanol steam reforming for hydrogen production: latest and effective catalyst modification strategies to minimize carbonaceous deactivation. Renew Sustain Energy Rev 74:89–103. https://doi.org/10.1016/j.rser.2017.02.049

23. Llorca J, Homs N, Sales J, de la Piscina PR (2002) Efficient production of hydrogen over supported cobalt catalysts from ethanol steam reforming. J Catal 209:306–317. https://doi.org/10.1006/jcat.2002.3643

24. Haga F, Nakajima T, Miya H, Mishima S (1997) Catalytic properties of supported cobalt catalysts for steam reforming of ethanol. Catal Lett 48:223–227. https://doi.org/10.1023/A:1019039407126

25. Cavallaro S, Mondello N, Freni S (2001) Hydrogen produced from ethanol for internal reforming molten carbonate fuel cell. J Power Sources 102:198–204. https://doi.org/10.1016/S0378-7753(01)00800-X

26. Greluk M, Rotko M, Słowik G, Turczyniak-Surdacka S (2019) Hydrogen production by steam reforming of ethanol over Co/CeO2 catalysts: effect of cobalt content. J Energy Inst 92:222–238. https://doi.org/10.1016/j.joei.2018.01.013

27. Llorca J, Homs N, Sales J, Fierro JLG, de la Piscina PR (2004) Effect of sodium addition on the performance of Co–ZnO-based catalysts for hydrogen production from bioethanol. J Catal 222:470–480. https://doi.org/10.1016/j.jcat.2003.12.008

28. Song H, Zhang L, Watson RB, Braden D, Ozkan US (2007) Investigation of bio-ethanol steam reforming over cobalt-based catalysts. Catal Today 129:346–354. https://doi.org/10.1016/j.cattod.2006.11.028

29. Courty Ph, Ajot H, Marcilly Ch, Delmon B (1973) Oxydes mixtes ou en solution solide sous forme très divisée obtenus par décomposition thermique de précurseurs amorphes. Powder Technol 7:21–38. https://doi.org/10.1016/0032-5910(73)80005-1

30. Kulawska M, Skrzypek J (2001) Kinetics of the synthesis of higher aliphatic alcohols from syngas over a modified methanol synthesis catalyst. Chem Eng Proc 40:33–40. https://doi.org/10.1016/S0255-2701(00)00107-0

31. Lachowska M (2010) Steam reforming of methanol over Cu/Zn/Zr/Ga catalyst: effect of the reduction conditions on the catalytic performance. Reac Kinet Mech Cat 101:85–91. https://doi.org/10.1007/s11144-010-0213-z

32. Szarawara J, Skrzypek J, Gawdzik A (1991) Podstawy inżynierii reaktorów chemicznych, 2nd edn. WNT, Warsaw

33. Kornas A, Grabowski R, Śliwa SK, Ruggiero-Mikołajczyk M, Żelazny A (2017) Dimethyl ether synthesis from CO2 hydrogenation over hybrid catalysts: effects of preparation methods. Reac Kinet Mech Cat 121:317–327

Publisher's Note Springer Nature remains neutral with regard to jurisdictional claims in published maps and institutional affiliations.